IJCRT.ORG ISSN : 2320-2882

INTERNATIONAL JOURNAL OF CREATIVE RESEARCH THOUGHTS (IJCRT)

An International Open Access, Peer-reviewed, Refereed Journal

Density Functional Theory Calculation Of Photophysical Properties Of 4-Hydroxy-4-Vinylpiperidine-1-Carbaldehyde Substituted Pyrazolone Analogue With Biological Functionalities

A. K. Maniyar[1], Doddamani Hanumanthanaik[2], Babu Giriya Gowda[3], Gousia Begum[4] and Kavitha B. S.[5]*

[1]Department of Physics, Mangalore University, Mangalagangotri, 574199 India and Department of physics, Government First Grade College Hubballi 580032. India
[2]Department of Chemistry, Government First Grade College Koppal-583231, India
[3]Department of Chemistry, Maharani Cluster University, Palace Road, Bangalore-56000, India
[4]Department of UG and PG Studies in Mathematics, Government (Autonomous) College Kalaburgi-585105 Karnataka, India
[5]Department of physics, Government Science College (Autonomous) Hassan-573201, India
Corresponding author Email id: kavitha.samu@gmail.com

Abstract:

In the present work, aryl-substituted pyrazolones derivative (E)-(5-(4-chlorophenyl)-1-(4-fluorophenyl)-1H-pyrazol-3-yl)(4-hydroxy-4-(prop-1-en-1-yl)piperidin-1-yl)methanone (5PPY) have been synthesized by the reaction of Baylis-Hillman acetate with pyrazolones and screened for their in vitro antifungal, antibacterial and antioxidant properties. The molecule shows good in vitro antifungal and antibacterial activities due to the presence of anisole, which enhances the absorption rate by its increased lipid solubility and improves the pharmacological activity. It is also evident from the results obtained from structure-activity relationship (SAR) studies. Insilico studies were conducted on the synthesized molecule, examining its interactions with DNA Gyrase, Lanosterol 14 alpha demethylase, and KEAP1-NRF2 proteins. The results revealed strong binding interactions at specific sites. Further, the photophysical properties of synthesized compounds were theoretical estimated using ab-intio technique. The ground state optimization, dipole moment and HOMO-LUMO energy levels are calculated using DFT-B3LYP-6-31G(d) basis set. Using theoretical estimated HOMO-LUMO value global chemical reactivity descriptors parameters are estimated and result shows synthesised molecule has highly

electronegative and electrophilicity index. The results suggest that, anisole substituted pyrazolones derivatives show good photophysical and biological applications.

Keywords: Pyrazolones, in-vitro and in-silico biological activity, HOMO-LUMO, MESP

1. Introduction

Recent developments in microbial resistance and the ongoing COVID-19 pandemic have intensified the quest for innovative antimicrobial and antiviral agents, spotlighting the significance of heterocyclic compounds like pyrazoles. These organic compounds, characterized by their carbon-nitrogen heterocycle, have attracted significant attention in biomedical research due to their diverse pharmacological properties. Notably, pyrazole derivatives have been explored for their potential in combating multidrug-resistant pathogens, including those associated with severe cases of COVID-19 necessitating antibiotic treatments. The pressing need for effective therapeutics against such microbial challenges underscores the importance of investigating pyrazole compounds and their biological activities [1-7].

Synthesis methods and structural modifications of pyrazole molecules have been extensively studied to enhance their pharmacological potential. For instance, research has focused on synthesizing ethyl 2-(3-methoxybenzyl) acrylate-substituted pyrazoles, aiming to explore their photophysical properties through advanced computational techniques like density functional theory (DFT) calculations. These computational studies offer insights into the electronic structure, stability, and spectroscopic characteristics of the synthesized pyrazole derivatives, aiding in understanding their potential applications in drug discovery and materials science [8-16].

Furthermore, recent advancements in pyrazole research have revealed intriguing photophysical phenomena exhibited by π-extended derivatives of pyrazoles. These compounds demonstrate strong blue-light emission and high quantum yields, making them attractive candidates for various applications in materials science and fluorescent probes for ion sensing. By modifying the π conjugation and incorporating specific substituents, researchers have been able to tailor the electronic properties of these pyrazole derivatives, enabling them to respond effectively to specific recognition events such as chelation with metals or interactions with anions [19-22]. This evolving understanding of pyrazole chemistry and its photophysical characteristics opens new avenues for designing functional materials and bioactive compounds with targeted properties for diverse applications in biomedical and materials research.

2. Materials and methods

The reagents employed were of high purity commercial samples which were used as received (Fischer, Merck, and Sigma Aldrich). Reactions were carried out in an oven-dried RB flask. TLC was performed on alumina silica gel 60F254 (Fischer) detected by UV light (254 nm) and iodine vapors. The melting points were determined by open capillaries on a Buchi apparatus and are uncorrected. The IR spectra were recorded on a

Nicolet-Impact-410 FT-IR spectrometer, using KBr pellets. ^{1}H-NMR and ^{13}C-NMR spectra were recorded on a Bruker AC-400F, 400MHz, spectrometer in DMSO-d_6 and $CDCl_3$ using TMS as an internal standard with the resonance frequency of 400 MHz and 100 MHz respectively. LCMS analyses were performed by using the Agilent 1200 series instrument. Elemental analysis was carried out by using Heraus CHN rapid analyzer. All the compounds gave C, H, and N analysis within ± 0.4% of the theoretical values.

2.1. **Synthesis of N/O-substituted pyrazalone derivatives**

The Compound (3) is synthesized through the combination of β-diketoester (1 mmol) and 4-fluorophenyl hydrazine (1 mmol) in a solution of 100 ml ethanol and 10 ml acetic acid. The mixture is refluxed overnight, after which the ethanol is removed by concentration, and the reaction mixture is subsequently neutralized with Na_2CO_3. The resulting solid is then filtered, dried, and further purified through recrystallization using ethanol. Further, pyrazole carboxylic acid ethyl ester (3), 1 mmol of the compound is dissolved in 50 ml of tetrahydrofuran (THF), followed by the addition of 15 ml of methanol, 20 ml of water, and 1.2 mmol of lithium hydroxide. The mixture is stirred overnight. Upon completion of the reaction, the solvent is concentrated to remove volatile components. The resulting residue is then dissolved in a solution comprising 50 ml of water and 100 ml of ethyl acetate. The solution is acidified to a pH of approximately 5 using 1N HCl. Subsequently, it is extracted with 100 ml of ethyl acetate twice. The combined organic layer is washed with 50 ml of water and a brine solution of 20 ml. Afterward, it is dried using Na_2SO_4 and evaporated to dryness resulting compound (4)

To the solution of (**4**) (1 mmol) in DCM (20 ml), oxalyl chloride (1.5 mmol) was added at 0°C, after 5 minutes catalytic amount of DMF (3 drops) was added and stirred at RT. After completion of the reaction, the reaction mixture was directly concentrated to remove excess of oxalyl chloride under nitrogen to get the neat acid chloride.

The acid chloride prepared was dissolved in fresh DCM (25 ml). Triethylamine (2 mmol) was added to the above solution at 0°C, followed by the addition of 4-piperidone (1.1 mmol) at 0°C. After completion of the reaction, reaction mixture was diluted with water (50 ml) and extracted with DCM (2×100ml), combined organic layer was washed with water (50 ml) and brine solution (20 ml) then dried over Na_2SO_4 and evaporated to dryness. Crude products were purified by washing with diethyl ether. To prepare compound (5), 1 mmol of the substance compound (4) is dissolved in 20 ml of dichloromethane (DCM). Then, 1.5 mmol of oxalyl chloride is added at 0°C, and after 5 minutes, a catalytic amount of dimethylformamide (DMF) in the form of 3 drops is introduced. The mixture is stirred at room temperature. Once the reaction is complete, the reaction mixture is directly concentrated under nitrogen to eliminate excess oxalyl chloride, resulting in the formation of the pure acid chloride. The acid chloride obtained is then dissolved in fresh DCM (25 ml). At 0°C, 2 mmol of triethylamine is added to the solution, followed by the addition of 1.1 mmol of 4-piperidone, also at 0°C. After the reaction is finished, the reaction mixture is diluted with 50 ml of water and extracted with DCM twice (2×100 ml). The combined organic layer is washed with 50 ml of water and a brine solution consisting of 20 ml. It is then dried with Na_2SO_4 and evaporated to dryness. To further purify the crude products, they are washed with diethyl ether.

Finally, 1mmol of compound (5) was taken in THF (20ml), and Grignard reagent (1.5mmol) at 0°C and after complete reaction, mass was allowed to attain RT. The reaction was monitored by TLC. The reaction the mixture was quenched with saturated ammonium chloride and extracted with ethyl acetate (2×100ml), combined organic layer was washed with water (50 ml) and brine solution (20 ml) then dried over Na_2SO_4 and evaporated to dryness. Crude products were purified by column chromatography using 230-400 silica gel.

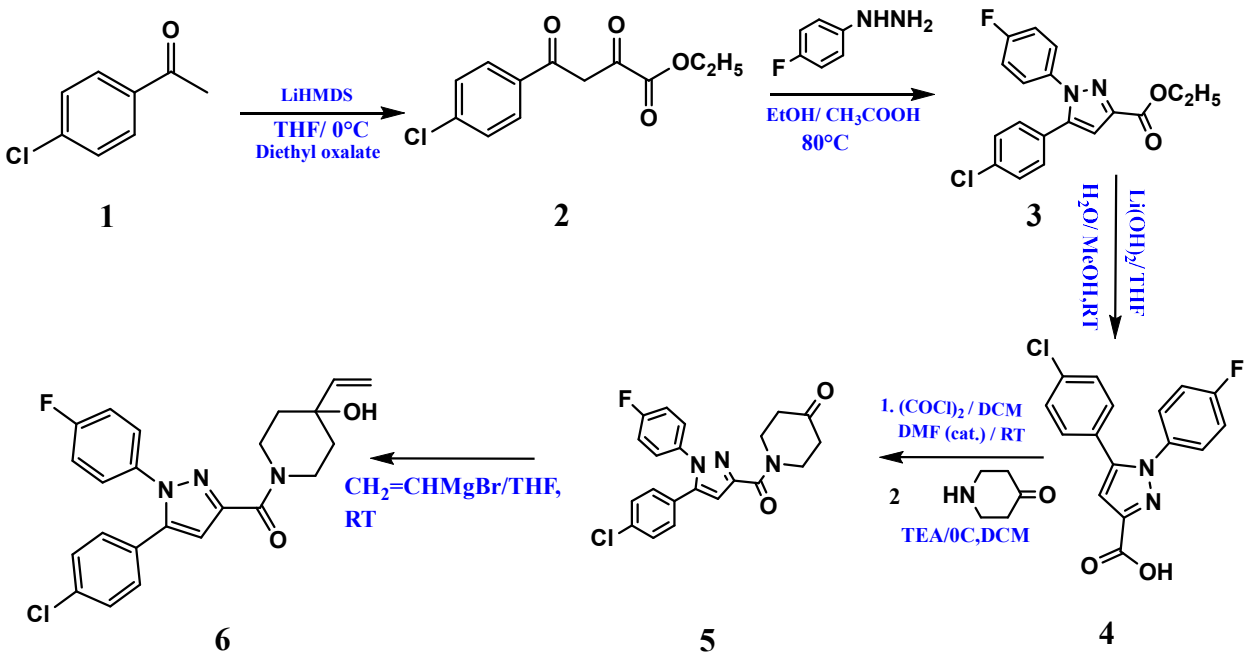

Scheme-1 synthesis of pyrazolone from Baylis-Hillman acetate.

2.2. **Structural characterization of the aryl-substituted pyrazolone (**5PPY**)**

White solid, mp 153.1^{0}C; % Yield: 98; ^{1}H NMR (400MHz, $CDCl_3$): δ= 7.27(d, 2H, ArH), 7.25(t, 2H, ArH), 7.16(dd, J= 4Hz, H-F_{Meta}, 2H, ArH), 7.07(dd, J= 8Hz, H-$F_{Ortho,}$ 2H, ArH), 6.88(s, 1H, pyrazole CH), 5.98(dd, J= 12Hz, 1H, =CH), 5.33(d, 1H, cis=CH_2), 5.14(d, 1H, trans =CH_2), 4.52(m, 2H, -CH_2), 3.69(m, 1H, -CH), 3.36(m, 1H, -CH), 1.87(m, 2H, -CH_2), 1.57(m, 2H, -CH_2); MS calcd.for $C_{23}H_{21}ClFN_3O_2$: 425.88, Found: 426.2(M +); IR (ν cm^{-1}): 3352(O-H), 3116(Ar-H), 2921(C-H), 1616(C=O); Elem. Anal. cald (found): C: 64.86(64.82), H: 4.97(4.96), N: 9.87(9.82).

3. Results and discussion

3.1. Density functional theory calculation for photophysical studies

Molecular orbitals and their properties, including energy levels, serve as valuable tools for physicists and chemists. These orbitals, especially the frontier electron density, are instrumental in predicting the most reactive positions within π-electron systems and elucidating various reactions in conjugated systems [23-25]. Additionally, the eigenvalues of the highest occupied molecular orbital (HOMO) and the lowest unoccupied

molecular orbital (LUMO), along with the energy gap between them, provide insights into the chemical reactivity of a molecule. Notably, the energy gap between the HOMO and LUMO has recently been employed to demonstrate the bioactivity resulting from intramolecular charge transfer (ICT) [26-27].

The ground state optimization of the newly synthesized 5PPY molecule was carried out using DFT-B3LYP/6-31G (d) basis set in Gaussian -09W software. The optimized molecular geometry and HOMO-LUMO energy plot of 5PPY were shown in Figs.1-2**.** From the HOMO-LUMO plot it is observed that, π–orbital of the HOMO electron cloud mainly distributes on 1-(4-fluorophenyl)-1H-pyrazole-3-carbaldehyde and unfilled π^*–orbital LUMO is on 5-(4-chlorophenyl)-1-(4-fluorophenyl)-1H-pyrazole-3-carbaldehyde

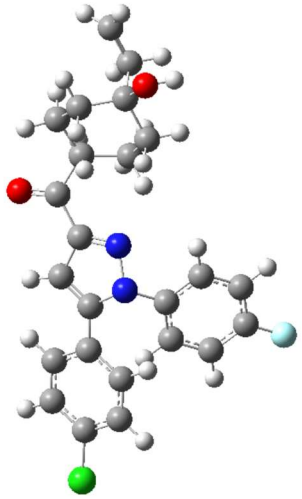

Fig.1. Optimised molecular geometry with atomic labels of the 5PPY molecule

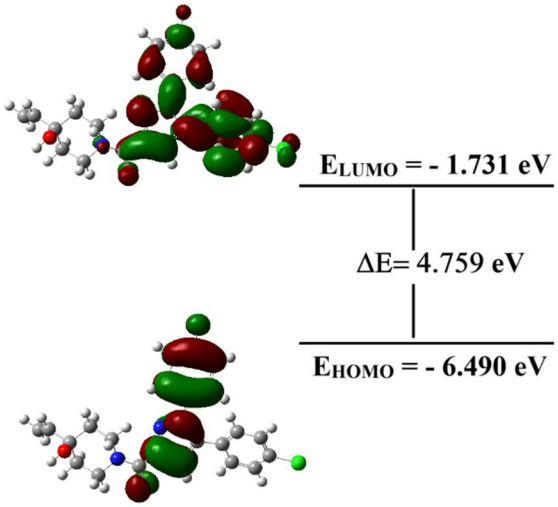

Fig.2. 3D plots of HOMO-LUMO with energy levels for 5PPY molecule

To gain insight on the chemical reactivity and stability of 5PPY molecules, global reactivity parameters [28], chemical hardness $(\eta = (IP - EA)/2) = 2.380eV$, electronegativity $(\chi = (IP + EA)/2) = 4.111eV$, chemical potential $(\mu = -\chi) = -4.11$ eV, chemical softness $(S = 1/2\eta) = 0.210$ eV and electrophilicity index $(\omega = \mu^2/2\eta)$

= 3.550 eV were calculated from E_{HOMO} and E_{LUMO} values [28], where, ionization potential, $IP = -E_{HOMO}$ = 6.490 eV and electron affinity, $EA = -E_{LUMO}$ = 1.731 eV. While a wider HOMO–LUMO gap is connected with stability and hardness, a lesser HOMO–LUMO gap signifies a more reactive soft molecule which is highly polarizable.

During molecular interactions, the lowest unoccupied molecular orbit (LUMO) accepts electrons and its energy corresponds to the electron affinity ($EA = -E_{LUMO}$), while the highest occupied molecular orbit (HOMO) represents electron donors, and its energy is associated with the ionization potential ($IP = -E_{HOMO}$). A molecule with a high frontier orbital gap (HOMO-LUMO energy gap) has a low chemical reactivity and high kinetic stability, because it is energetically unfavorable to add an electron to the high-lying LUMO in order to remove electrons from the low-lying HOMO. For instance, compounds that have a high HOMO-LUMO energy gap are stable, and hence are chemically harder than compounds having a small HOMO-LUMO energy gap. Thus, from GCRD parameter, that compound 5PPY is hard and more stable (less reactive) and it may be due to substitution of (E)-4-hydroxy-4-(prop-1-en-1-yl)piperidine-1-carbaldehyde linked in non-planar to pyrazole and produce the highest energy gap. Thus, these substituents increase the reactivity of the five-membered ring.

The deformation of the molecular electron cloud is visible under mild perturbation due to the resistance that offers hardness throughout the chemical process. Hard molecules are comparatively small and significantly less polarizable than soft molecules, which are big and highly polarizable. The molecules stability and intermolecular reactivity are shown by the hardness. While softness exhibited an inverse effect with respect to hardness. The ability of additional electrical charge acquired by the electrophile is related to electrophilicity phenomena. The information regarding chemical potential (electron transfer) and hardness of molecule (stability) were provided by the opposition to the exchange charge of an electron with nature. One of the most crucial quantum chemical descriptors for determining the toxicity of compounds in terms of their reactivity and site selectivity is the electrophilicity index [28]. According to HOMO-LUMO energy values, the electrophilicity index measures the reduction in energy brought on by the maximum amount of electron flow between the donor and acceptor. The lower value of ω indicated a good nucleophile, one with a higher ω value is considered a good electrophile. If any organic molecule is considered to be a strong electrophile the electrophilicity ω scale value should be $\omega > 1.5$ eV. If the scale varies between $0.8 < \omega < 1.5$ eV then those are considered as moderate electrophile and electrophile with electrophilicity value $\omega < 0.8$ eV are the weaker ones [29-30]. Our findings suggest that the 5PPY described here are better electrophiles because they have a higher value of ω. The propensity of electrons to leave a stable system is described as the chemical potential (μ). A complex has a negative chemical potential value if it is stable and does not spontaneously break into its constituent components. The 5PPY molecule do not break down into elements, as evidenced by their negative chemical potentials. The HOMO-LUMO gap support for chemical hardness at energy of 4.055 eV shows that this energy is less polarizable and resist the deformation of the chemical systems electron cloud under moderate disturbances.

3.1.1. Molecular electrostatic potential map (MESP) estimated using DFT analysis

The MESP is a valuable parameter linked to electron density, offering insights into sites conducive to electrophilic and nucleophilic reactions, as well as hydrogen bonding interactions. Moreover, MESP is highly relevant for studying processes where one molecule interacts with another, such as in drug-receptor and enzyme-substrate interactions. This interaction begins with the recognition of the two species through their electrostatic potentials. To pinpoint the reactive sites for electrophilic and nucleophilic attacks in the molecule under investigation, we calculated the MESP at the optimized geometry using DFT-B3LYP/6-31G(d). Different colors on the MESP surface correspond to distinct electrostatic potential values: red indicates regions with the most negative potential, blue represents the most positive regions, and green signifies areas with zero electrostatic potential. Negative electrostatic potential, characterized by shades of red, indicates regions where protons are attracted to the electron density within the molecule. In contrast, positive electrostatic potential, seen in shades of blue, indicates regions where protons are repelled by atomic nuclei. Specifically, the negative (red and yellow) regions of the MEP denote electrophilic reactivity, while the positive (blue) regions signify nucleophilic reactivity (see Fig. 3). Upon examining the MEP, it becomes evident that the negative charge predominantly covers the pyrazole, while the positive region is concentrated over the hydroxyl group and the N-H section. The higher electronegativity of the nitro group renders it the most reactive part of the molecule [20].

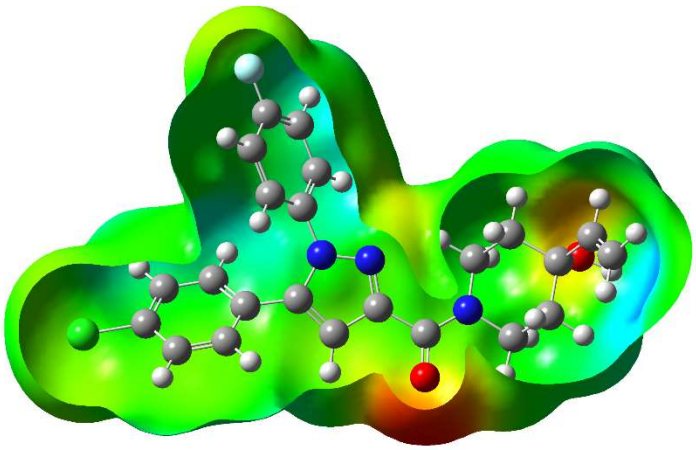

Fig.3. Molecular electrostatic potential map of 5PPY molecule

3.2. **In vitro antimicrobial, antifungal, and antioxidant activity**

The newly synthesized molecule 5PPY were subjected to antimicrobial studies and interestingly, the compound exhibited perfect antibacterial activity against S.aureus, B.subtillis, S.typhi, and E.coli and details are given in Table-1. In addition, 5PPY molecule also exhibited very good antifungal activity against A. niger and C. Albicans and details are given Table 1. The better activity of the products could be due to the presence of biologically active pyrazole and bromo benzene ring. Bromobenzene is the second smallest substituent, which resembles hydrogen with respect to steric requirements at enzyme receptor sites. The presence of bromine enhances the absorption rate by its increased lipid solubility [29]. The high lipophilic character of the bromobenzene group is significant in improving pharmacological activity. Further, antioxidant activity of the 5PPY molecules was screened and showed excellent radical scavenging capacity at the tested concentration of

15 µg/mL in comparison with the standard edaravone as shown in Table 2. The variation exhibited in DPPH scavenging capacity could be attributed to the effect of different substitutions at 1, 2, 3 and 5 of the synthesized compounds. The antioxidant activity results are in the range as observed in the previous results [30].

Table -1 Antimicrobial and antifungal activity of the newly synthesized pyrazolones derivatives

Compound	S. aureus	B. subtilis	S. typhi	E. coli	A. niger	C. albicans
5PPY	25	27	28	29	23	25
Standard	24	23	23	25	25	24
Control DMSO	0	0	0	0	0	0

Note: Standard drug used: Bacteria (Ciprofloxacin), Fungal (Fluconazole) were in 40 µg in 100µL
[b]Control: DMSO (Dimethyl sulphoxide)

Table-2 DPPH scavenging assay of aryl substituted pyrazolones derivatives.

Compounds Concentration (15µg/mL)	5PPY	Standard (edaravone)
% DPPH scavenging	54.87	73.16

4. Conclusions

In the present work, we synthesised highly functionalized aryl-substituted pyrazolone derivatives (5PPY). The physicochemical properties of the 5PPY are confirmed by ^{1}H-NMR, FT-IR and LC-MS data. The photophysical properties of the compounds were comprehensively estimated using computational technique. The optimised molecular geometry, HOMO-LUMO and MESP plot of the 5PPY molecule are estimated using DFT-B3LYP-6-31G(d) basis set. Using theoretical estimated HOMO-LUMO values global chemical reactive descriptor parameters is estimated and results shows that 5PPY molecule has a good electrophile, highlighting its reactivity and relatively lower stability. Electron-deficient sites in 5PPY were identified through DFT calculation studies, which can be utilized in the design of drugs for biological applications. Furthermore, the in-vitro antimicrobial, antifungal and antioxidant activities of the 5PPY molecule was examined and results shows that molecule has high biological application. Overall, the results indicate that the 5PPY could be used as biological and optoelectronic applications.

Reference

1. Breijyeh, Z., Jubeh, B., & Karaman, R. Resistance of gram-negative bacteria to current antibacterial agents and approaches to resolve it. Molecules, 25(6), (2020) 1340.
2. Balasubramaniam, B., Prateek, Ranjan, S., Saraf, M., Kar, P., Singh, S. P., & Gupta, R. K. Antibacterial and antiviral functional materials: chemistry and biological activity toward tackling COVID-19-like pandemics. ACS Pharmacology & Translational Science, 4(1), (2020) 8.

3. Nasir, N., Rehman, F., & Omair, S. F. Risk factors for bacterial infections in patients with moderate to severe COVID-19: A case-control study. Journal of medical virology, 93(7), (2021) 4564.
4. Becerra, D., Abonia, R., & Castillo, J. C. Recent applications of the multicomponent synthesis for bioactive pyrazole derivatives. Molecules, 27(15), (2022) 4723
5. Özlem, U. Ğ. U. Z., Gümüş, M., Yusuf, S. E. R. T., İrfan, K. O. C. A., & Atıf, K. O. C. A. Utilization of pyrazole-perimidine hybrids bearing different substituents as corrosion inhibitors for 304 stainless steel in acidic media. Journal of Molecular Structure, 1262, (2022) 133025.
6. Özkınalı, S., Gür, M., Şener, N., Alkın, S., & Çavuş, M. S. Synthesis of new azo schiff bases of pyrazole derivatives and their spectroscopic and theoretical investigations. Journal of Molecular Structure, 1174, (2018). 74-83.
7. Khoram, M. M., Nematollahi, D., Momeni, S., Zarei, M., & Zolfigol, M. A. Electrochemical study of dibenzo-xanthene and dihydrobenzochromono pyrazole derivatives. Electrochimica Acta, 326, (2019) 134990.
8. Gao, M., Qu, K., Zhang, W., & Wang, X. Pharmacological activity of pyrazole derivatives as an anticonvulsant for benefit against epilepsy. Neuroimmunomodulation, 28(2), (2021) 90.
9. Santos, N. E., Carreira, A. R., Silva, V. L., & Braga, S. S. Natural and biomimetic antitumor pyrazoles, a perspective. Molecules, 25(6), (2020) 1364.
10. Datar, P. A., & Jadhav, S. R. Design and synthesis of pyrazole-3-one derivatives as hypoglycaemic agents. International Journal of Medicinal Chemistry, 2015 (2015).
11. Cetin, A., & Bildirici, I. A study on synthesis and antimicrobial activity of 4-acyl-pyrazoles. Journal of Saudi Chemical Society, 22(3), (2018) 279.
12. Uramaru, N., Shigematsu, H., Toda, A., Eyanagi, R., Kitamura, S., & Ohta, S. Design, synthesis, and pharmacological activity of nonallergenic pyrazolone-type antipyretic analgesics. Journal of medicinal chemistry, 53(24), (2010) 8727.
13. Desideri, N., Fioravanti, R., Proietti Monaco, L., Atzori, E. M., Carta, A., Delogu, I., & Loddo, R. Design, Synthesis, Antiviral evaluation, and SAR studies of new 1-(phenylsulfonyl)-1 H-pyrazol− 4-yl-methylaniline derivatives. Frontiers in chemistry, 7, (2019) 214.
14. Pandya, K. M., Patel, A. H., & Desai, P. S. Development of Antimicrobial, Antimalarial and Antitubercular Compounds Based on a quinoline-pyrazole clubbed scaffold derived via Doebner reaction. Chemistry Africa, 3, (2020) 89.
15. Zalaru, C., Dumitrascu, F., Draghici, C., Iovu, M., Marinescu, M., Tarcomnicu, I., Nitulescu, G.M. Synthesis and biological screening of some novel 2-(1H-pyrazol-1-yl)-acetamides as lidocaine analogue. Indian J. Chem. B 53, (2014) 733
16. Refat, M. S., Hamza, R. Z., Adam, A. M. A., Saad, H. A., Gobouri, A. A., Al-Salmi, F. A., & El-Megharbel, S. M. Synthesis of N, N′-bis (1, 5-dimethyl-2-phenyl-1, 2-dihydro-3-oxopyrazol-4-yl) sebacamide that ameliorate osteoarthritis symptoms and improve bone marrow matrix structure and

cartilage alterations induced by monoiodoacetate in the rat model:"Suggested potent anti-inflammatory agent against COVID-19". Human & Experimental Toxicology, 40(2), (2021) 325.

17. Flamholc, R., Zakrzewski, J., Makal, A., Brosseau, A., & Métivier, R. Synthesis, regioselective aerobic Pd (II)-catalyzed C–H bond alkenylation and the photophysical properties of pyrenylphenylpyrazoles. Photochemical & Photobiological Sciences, 15(4), (2016) 580.
18. Castillo, J. C., & Portilla, J. Recent advances in the synthesis of new pyrazole derivatives. Targets Heterocycl. Syst, 22, (2018) 194.
19. Beillard, A., Bantreil, X., Métro, T. X., Martinez, J., & Lamaty, F. Alternative technologies that facilitate access to discrete metal complexes. Chemical reviews, 119(12), (2019) 7529.
20. Beneto, A. J., & Siva, A. Highly selective colorimetric detection of cyanide anions in aqueous media by triphenylamine and phenanthro (9, 10-d) imidazole based probes. Photochemical & Photobiological Sciences, 16, (2017) 255.
21. Naskar, B., Das, K., Mondal, R. R., Maiti, D. K., Requena, A., Cerón-Carrasco, J. P., & Goswami, S. A new fluorescence turn-on chemosensor for nanomolar detection of Al^{3+} constructed from a pyridine–pyrazole system. New Journal of Chemistry, 42(4), (2018) 2933.
22. A.H. Collins, Microbiological Methods, 2nd Edition, Butterworth, London, 1976.
23. Arthington-Skaggs, B. A., Motley, M., Warnock, D. W., & Morrison, C. J. Comparative evaluation of PASCO and national committee for clinical laboratory standards M27-A broth microdilution methods for antifungal drug susceptibility testing of yeasts. Journal of Clinical Microbiology, 38(6), (2000) 2254.
24. Naik, L., Maridevarmath, C. V., Khazi, I. A. M., & Malimath, G. H. Photophysical and computational studies on optoelectronically active thiophene substituted 1, 3, 4-oxadiazole derivatives. Journal of Photochemistry and Photobiology A: Chemistry, 368, (2019) 200
25. Walki, S., Malimath, G. H., Mahadevan, K. M., Naik, S., Sutar, S. M., Savanur, H., & Naik, L. Synthesis, spectroscopic properties, and DFT correlative studies of 3, 3′-carbonyl biscoumarin derivatives. Journal of Molecular Structure, 1243, (2021). 130781.
26. Prabhala, P., Sutar, S. M., Manjunatha, M. R., Pawashe, G. M., Gupta, V. K., Naik, L., & Kalkhambkar, R. G. Synthesis, in vitro and theoretical studies on newly synthesized deep blue emitting 4-(p-methylphenylsulfonyl-5-aryl/alkyl) oxazole analogues for biological and optoelectronic applications. Journal of Molecular Liquids, 360, (2022) 119520.
27. Naik, L., Thippeswamy, M. S., Praveenkumar, V., Malimath, G. H., Ramesh, D., Sutar, S., & Bubbly, S. G. Solute-solvent interaction and DFT studies on bromonaphthofuran 1, 3, 4-oxadiazole fluorophores for optoelectronic applications. Journal of Molecular Graphics and Modelling, 118, (2023) 108367.
28. Calais, J. L. (1993). Density-functional theory of atoms and molecules. RG Parr and W. Yang, Oxford University press, New York, Oxford, International Journal of Quantum Chemistry, 47(1), (1989) 101.

29. Choudhary, V., Bhatt, A., Dash, D., & Sharma, N. DFT calculations on molecular structures, HOMO–LUMO study, reactivity descriptors and spectral analyses of newly synthesized diorganotin (IV) 2-chloridophenylacetohydroxamate complexes. Journal of computational chemistry, 40(27), (2019) 2354.
30. Yankova, R., & Tankov, I. NLO response as a function of structural water presence: A comparative experimental (UV-vis) and DFT (structural, NPA, MEP) study on Cs_2Ni (SeO_4) 2• $4H_2O$ and Cs_2Ni (SeO_4) 2. Journal of Molecular Structure, 1224, (2021) 129047.